Comparison between RANS and LES Approaches to the Simulation of Natural Convection in a Differentially Heated Square Cavity

MATTEO PACHERA*,[1], PIERFRANCESCO BRUNELLO*,[2], MARCO RACITI CASTELLI♯,[3]

* Department of Industrial Engineering
University of Padua
Via Venezia 1, 35131 Padua
ITALY
♯ Department of Management and Engineering
University of Padua
Stradella S. Nicola 3, 36100 Vicenza
ITALY

[1]matteo.pachera@dii.unipd.it; [2] pierfrancesco.brunello@unipd.it; [3] marco.raciticastelli@unipd.it

Abstract: The capabilities of Fire Dynamics Simulator (FDS), a LES code for fire dynamics assessment, to correctly predict also a buoyancy driven flow in a small square cavity are discussed and compared with the results of a well established CFD solver (Ansys Fluent). In both cases, numerical predictions are compared with a detailed experimental benchmark available in the literature, where the flow field in a 0.75 m high, 0.75 m wide and 1.5 m deep cavity was extensively measured. Both the hot wall of the cavity and the cold one were isothermal (respectively at $50\ ^{\circ}C$ and $10\ ^{\circ}C$), giving a Rayleigh number of 1.58×10^9. A quite remarkable agreement between numerical and experimental data is obtained using Ansys Fluent, while new values of the coefficients for natural convection in FDS are hereby proposed, allowing a significant improvement of the capabilities of the code to reproduce the experimental heat transfer.

Keywords: CFD; natural convection; buoyancy driven flow; FDS; Ansys Fluent.

1 Introduction

Natural convection in enclosures is a physical phenomenon which often occurs in engineering problems, such as building, furnace and cooling tower simulations, as well as the simulation of electronic cooling systems. The resulting flow field and heat transfer were studied in scaled test facilities (mainly characterized by very simple geometries) [1] [2] [3] and through numerical simulations [4]. Many of them concern with two-dimensional square cavities with differentially heated vertical walls and horizontal insulated walls [5] [6] [7] [8]. Several studies were also performed in order to define some engineering correlations for heat transfer calculation, starting from the Rayleigh number [9].

Buoyancy driven flows find applications also in large scale problems: in fact, with the ongoing development of large hotel atriums and halls, it become fundamental the investigation of air motion within confined large spaces [10] [11].

New building technologies, such as double skin glasses and double skin facades [12] [13], which allow a great energy saving, also require the study of the flow field inside enclosures. In such applications, smoke and hot gas movement in case of fire are driven by buoyancy forces and should be thoroughly understood in order to predict the smoke pattern and design the exhaust process [14].

As well known, Computational Fluid Dynamics (CFD) codes are increasingly popular for analysing and predicting thermo-fluid dynamics phenomena in very different conditions. Some codes are well-established and general purpose (e.g. Ansys Fluent), others instead are devoted to specific problems. This is the case of Fire Dynamics Simulator (FDS), since it was developed and optimized to simulate fires in large scale buildings and tunnels, resorting to the Large Eddy Simulation (LES) approach. However, at least in principle, the numerical core of the program could be used also in different conditions. Thus, the purpose of this work is to assess the applicability of FDS to a very different problem, such as the prediction of natural convection in a differentially heated small square

cavity. For this case, very reliable experimental data are available in the literature.

The obtained numerical results are successively compared also with a well established commercial CFD solver (Ansys Fluent). The comparison shows how the two codes, which are characterized by a completely different approach to the numerical problem - a steady-state Reynolds Averaged Navier Stokes (RANS) simulation is hereby proposed for Ansys Fluent, while a LES approach is adopted for FDS - can nevertheless produce accurate results, provided a new value of the coefficient for natural convection in FDS is implemented. The hereby proposed value is based on the work of Ampofo and Karayannis [8]; further validations should nevertheless be performed in order to definetively confirm such a value.

2 Considered benchmark

The experimental data adopted for the validation of the hereby presented numerical simulations were obtained from [8]. As shown in Figure 1, a box 0.75 m high (z-axis) 0.75 m wide (x-axis) and 1.5 m deep (y-axis), containing air at atmospheric pressure, was heated from one side (the left wall) and cooled from the other one (the right wall) to generate a circular flow patter in the air. This geometry was designed to provide a 2-D flow field at the vertical plane in the middle of the cavity: in fact, as pointed out by Penot and N'Dame [15], if the horizontal aspect ratio is greater than 1.8, the three dimensional effects can be neglected.

The vertical walls were kept at constant temperatures of 50° C and 10° C respectively by pumping water with a rate of 40 l/min inside water gaps separated from the air by a 6 mm steel plate.

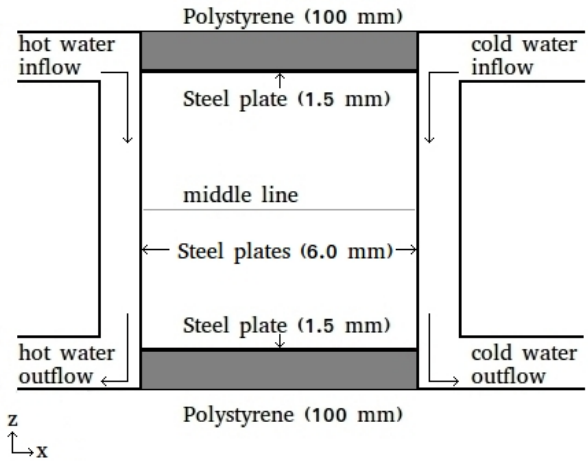

Figure 1: Experimental set-up used by Ampofo and Karayannis [8]

The horizontal walls were made by a 1.5 mm mild steel sheet, coated with a 100 mm polystyrene layer, insulating the cavity from the laboratory where the air temperature was 30° C constant. The front and rear walls were made by a double glass panel and were used as guard cavities.

In steady conditions, velocities and temperatures were measured at different positions on the vertical middle plane (y = 0.75 m). A laser Doppler anemometer (LDA) was employed to measure the instantaneous velocities, while micro-diameter thermocouples were used to measure the air temperatures, as well as the surface temperatures of the walls. These data were used to compute the local Nusselt number along the surfaces, using the following expression:

$$Nu_{loc} = -\frac{H}{T_h - T_c}\frac{\partial \overline{T}}{\partial x_i}\bigg|_w \qquad (1)$$

where H was the width of the cavity, T_h and T_c were the hot wall and cold wall temperatures, and the derivative was evaluated on the wall in the thermal boundary layer using the local surface temperature and the air temperature inside the conductive layer.

3 FDS numerical approach

As well known, Fire Dynamics Simulator (FDS) is a CFD code developed by the National Institute of Standards and Technology (NIST) and by the Technical Research Centre of Finland (VTT) [16]. FDS is a LES code for low-speed flows, with an emphasis on smoke and heat transport from fires in large scale domains. Unlike other CFD codes which can be employed to simulate different physical problems using a general approach, FDS was developed for this specific application and many features are enhanced to properly simulate fire phenomena.

The LES approach, firstly developed by Smagorinsky [17], is based on the application of Kolmogorov's (1941) theory about self similarity. The large eddies of the flow are dependent on the geometry, while the smaller scales are not strictly dependent on that. Hence the large eddies are explicitly solved in the calculation, while the small eddies are implicitly accounted for, by using a subgrid-scale model (SGS model).

FDS is a structured, uniform grid solver, since these perform more stable calculations and reduce the error propagation through the cells [18]. The usage of an uniform mesh does not allow to generate a really thin grid spacing near the wall unless using very fine grids. Thus, to avoid too heavy calculations, the flow inside the boundary layer is not explicitly solved since it is usually contained in the first

cells row, but the near-wall velocities in the first cell are calculated by means of the correlations of Werner and Wengle [19], whereas the viscous stress is modelled using a logarithmic velocity profile. Near the wall, the tangential velocities are in phase with the instantaneous wall shear stress and the friction velocity is assumed to have a profile which is linear in the first region ($y^+ < 11.81$) and logarithmic elsewhere ($y^+ > 11.81$). The near wall velocity is calculated from the wall shear stress, integrating the friction velocity profile along the height of the first cell.

The convective heat transfer between a wall and the fluid is also modelled with a simplified approach: instead of solving the thermal boundary layer and using the local conduction in the first cell, a convective heat transfer coefficient *h* is used for the first cell; this coefficient is calculated by resorting to a combination of natural and forced convection correlations, which allows to obtain a good prediction of the heat transfer within the correct range of y^+ values:

$$q_c = h(T_g - T_w) \tag{2}$$

$$h = max\left[C_1|T_g - T_w|^{\frac{1}{3}}; \frac{k}{L}Nu\right] \tag{3}$$

$$Nu = C_2 + C_3 \cdot Re^n \cdot Pr^m \tag{4}$$

where C_1, C_2 and C_3 are suitable coefficients depending on the geometry, Re and Pr are Reynolds and Prandtl numbers respectively, T_g is the gas temperature in the first cell, T_w is the wall temperature, k is the gas conductivity and L is a characteristic length [20] [21].

4 FDS numerical set-up

Since the aspect ratio of the cavity allows to neglect the three dimensional effects, a 2-D calculation was performed, assuming a infinitely deep cavity. For the hot and the cold walls the temperature was defined as constant ($50°C$ and $10°C$ respectively), according to the experimental results. As for the upper and lower surfaces, the wall described in [8] was implemented in the model, with 1.5 mm of mild steel and 100 mm of polystyrene facing the room at $30°C$. The properties of such materials were not explicitly defined in [8], so they were assumed as shown in Table 1.

A default fully structured mesh was initially implemented using a grid of 400 elements (20x20), thus giving a maximum y^+ of 27.5. The standard radiation model used by FDS was not modified, with an emissivity of the surfaces equal to 0.9.

The LES approach implies transient simulations, hence to have steady state conditions as in the experiment, the simulated time was 1000 s, which was long enough to stabilise the fluid quantities and consider the simulation steady state. The initial conditions of the air in the cavity were taken from [8]: temperature $30°C$, velocity 0 m/s and relative pressure 0 Pa.

Table 1: Thermal properties of upper and lower walls

Material	steel	polystyrene
Thickness [m]	0.0015	0.1
Conductivity [W/m/K]	45	0.033
Specific heat [kJ/kg/K]	0.45	1.3
Density [kg/m^3]	7800	50

The fluid inside the cavity was air with temperature dependent thermo-physical properties.

5 FDS Results and discussion

As expected, the simulations always showed a circular flow pattern in the vertical middle plane, with an ascending layer close to the hot wall (on left-hand side of Figure 2) and a descending one on the opposite side. In the central part of the analysed domain, the velocity values were always negligible.

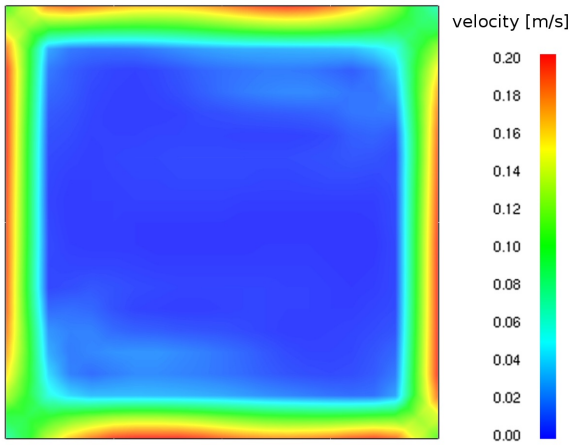

Figure 2: Example of flow pattern (scale of flow absolute velocity in m/s)

Therefore, the comparisons with the benchmark were carried out referring to four quantities: vertical velocity and temperature at the middle line (see Figure 1), specific convective heat transfer along hot and cold walls.

As for the experiments, the convective heat transfer per unit of area q was hereby computed from the local Nusselt number by resorting to the expression:

$$q = \frac{Nu_{loc}}{L}k(T_h - T_c) \tag{5}$$

being L the cavity length (0.75 m) and the Nusselt

provided in [8]. For the numerical simulations, q simply derives from:

$$q = h(T_w - T_g) \tag{6}$$

where the convective coefficient h is given by eq. (3), T_w is the temperature of the wall and T_g is the temperature of the gas in the first cell near the surface.

The comparison between the above mentioned quantities and the corresponding experimental values are shown in Figures from 3 to 6. In each figure, in addition to the experimental values and to the numerical results obtained as previously described, another set of data is provided. This set of data was obtained assigning to the upper and lower surfaces the temperature profiles measured in [8]. In order to assess the possible consequences of the uncertainties on the structure on these walls.

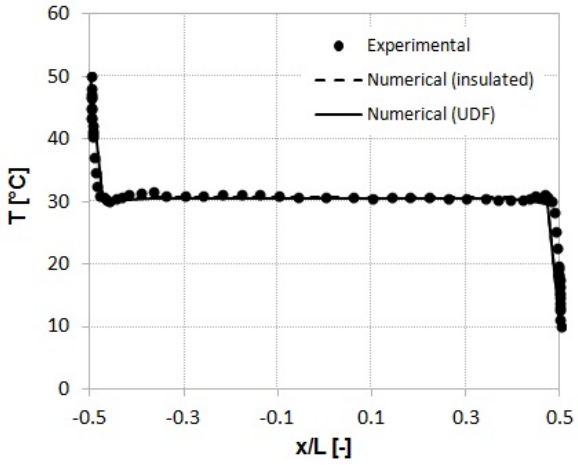

Figure 3: Temperature profile at the middle line (20x20 mesh resolution)

Looking at the results, while the temperature profile along the middle line shows a remarkable agreement between measured and numerically predicted values, significant discrepancies can be observed for the vertical velocity profile and, even more, for the specific convective heat transfer.

The comparison between maximum and minimum velocities and to convective heat fluxes at the vertical walls is presented in Table 2, where the numerical results are obtained with assigned upper and lower surface temperatures, as previously described.

As for vertical velocity, the observed shift in x-direction of the peaks is to be ascribed to the huge near-wall cell dimension, necessary to obtain the prescribed value of $y^+ = 30$, allowing FDS to have a well resolved flow. Nevertheless, the considered geometry may require a smaller cell dimension, in order to simulate the region near the wall and to define a more accurate velocity profile.

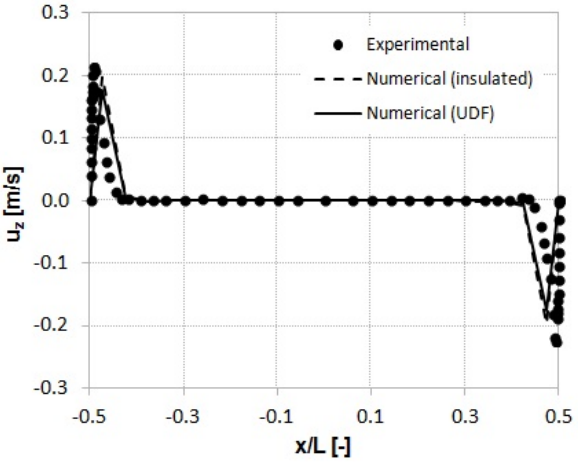

Figure 4: Vertical velocity profile at the middle line (20x20 mesh resolution)

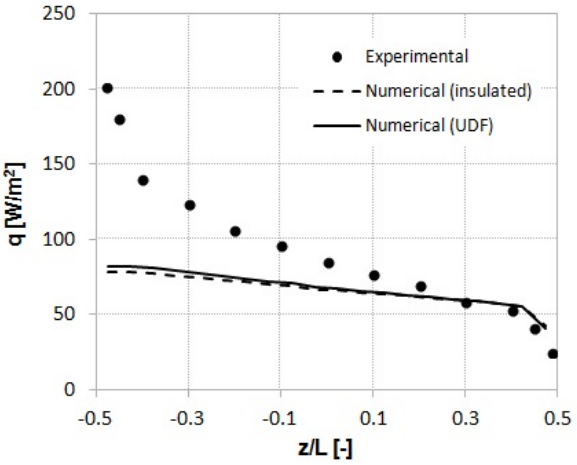

Figure 5: Specific convective heat transfer along the hot wall (20x20 mesh resolution)

Table 2: Comparison between representative data (20x20 mesh resolution)

	experimental	numerical
$u_{z,max}$	0.213 m/s	0.177 m/s
$u_{z,min}$	- 0.226 m/s	- 0.176 m/s
q_{hot}	105.04 W	76.35 W
q_{cold}	- 93.95 W	- 76.93 W

In order to verify such assumption, a fully structured mesh was implemented using a grid of 6400 elements (80x80), thus giving a maximum y^+ of 8.23. As can be drawn from Figure 7, the resulting vertical velocity profile shows, in this case, a remarkable agreement with experimental measurements, but the specific convective heat transfer still remains underestimated, giving even worse predictions with respect to

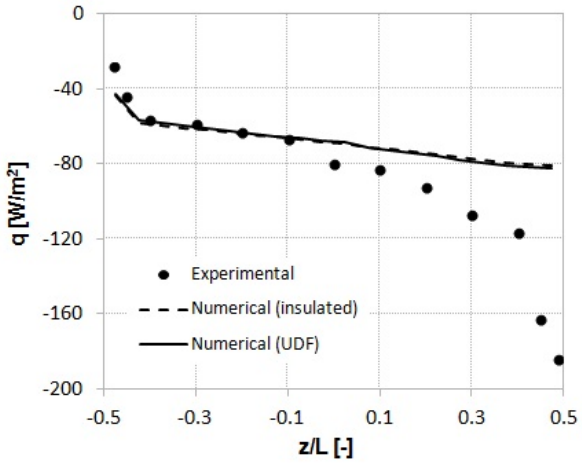

Figure 6: Specific convective heat transfer along the cold wall (20x20 mesh resolution)

the previous ones (see Figure 8 and Table 3).

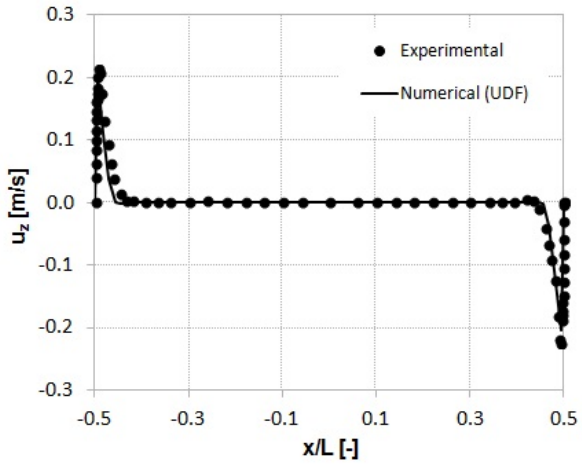

Figure 7: Vertical velocity profile at the middle line (80x80 mesh resolution)

Table 3: Comparison between representative data (80x80 mesh resolution)

	experimental	numerical
$u_{z,max}$	0.213 m/s	0.201 m/s
$u_{z,min}$	- 0.226 m/s	- 0.205 m/s
Q_{hot}	105.04 W	60.58 W
Q_{cold}	- 93.95 W	- 61.72 W

Then, in order to match the experimental heat transfer, the default values of the coefficient C_1 for natural convection, used in eq. 3, was modified (from 1.52 to 2.80 for horizontal surfaces and from 1.31 to 1.80 for vertical surfaces). Again, a 20x20 mesh resolution was adopted, in order to obtain the prescribed

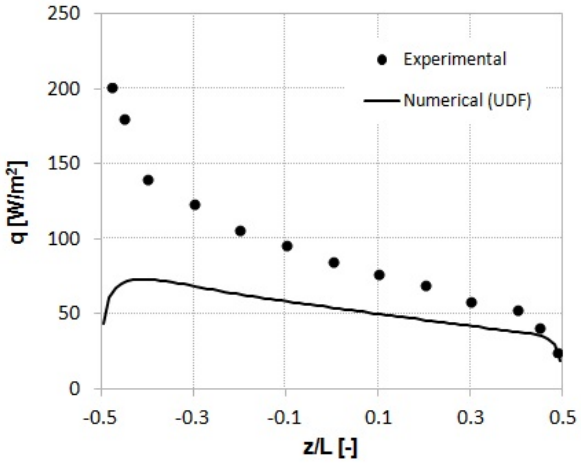

Figure 8: Specific convective heat transfer along the hot wall (80x80 mesh resolution)

value of $y^+ = 30$.

In this way, the agreement with the experimental results significantly improves as shown in Table 4. As shown in Figure 9 and Figure 10, some discrepancies still remain for the local heat transfer q on the hot and cold walls, but the overall heat flux Q on a wall is usually of major interest for technical applications.

Table 4: Comparison between representative data (20x20 mesh resolution, modified C_1)

	experimental	numerical
$u_{z,max}$	0.213 m/s	0.213 m/s
$u_{z,min}$	- 0.226 m/s	- 0.211 m/s
Q_{hot}	105.04 W	103.53 W
Q_{cold}	- 93.95 W	- 103.95 W

6 Ansys Fluent numerical set-up

The experimental data from [8] were successively compared with the numerical predictions of a robust and widely accepted commercial CFD package (Ansys Fluent). In the present formulation, the CFD code adopted the Reynolds Averaged Navier Stokes (RANS) equations, that are far too known to be reported here again. The non-linear govering equations for the conservation of mass, momentum and turbulence were solved sequentially (i.e., segragated from one another) by the numerical code, which is based on a finite volume method. The governing equations were implicitly discretized by a second-order upwind scheme and linearized to determine a system of equations for the dependent variables in every computational cell. The resulting linear system produced a

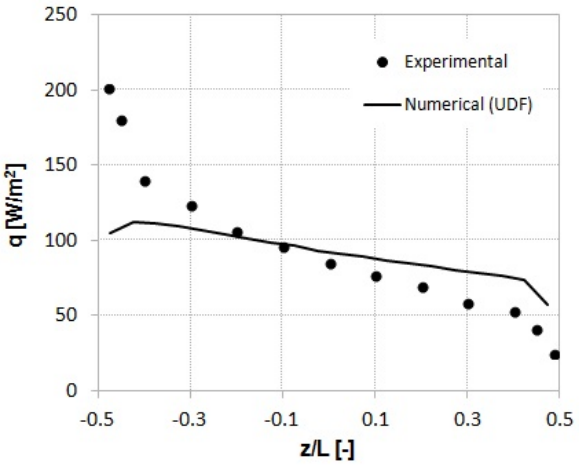

Figure 9: Specific convective heat transfer along the hot wall (20x20 mesh resolution, modified coefficients for natural convection)

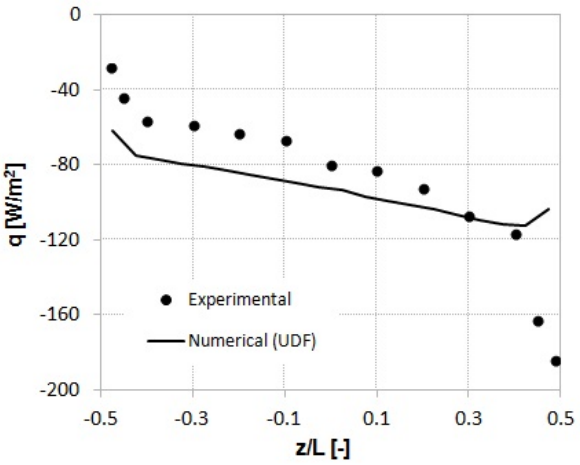

Figure 10: Specific convective heat transfer along the cold wall (20x20 mesh resolution, modified coefficients for natural convection)

sparse coefficient matrix whose solution produced the updated flow field.

The *Standard k-ε* turbulence model, coupled to the *Standard Wall Function* option, provided the best outcome in the numerical results and was therefore chosen for the present simulations. Default under-relaxation factors are adopted to suppress oscillations of the solution (Table 5).

Once more, a 2-D calculation was performed, assuming an infinitely deep cavity. Constant temperatures (of 50 $^{\circ}C$ and 10 $^{\circ}C$ respectively) were assumed for the hot and cold walls, while the experimental profile temperatures of both upper and lower surfaces were assigned using appropriate User Defined Functions (UDFs), thus allowing a full control

Table 5: Adopted under-relaxation factors (default values)

Pressure [-]	0.3
Density [-]	1.0
Body forces [-]	1.0
Momentum [-]	0.7
Turbulent kinetic energy [-]	0.8
Turbulent dissipation [-]	0.8
Turbulent viscosity [-]	1.0
Energy [-]	0.6

of the boundary conditions even though the real physical properties of the surfaces were not implemented in the numerical model.

Contrarily to the case of the FDS simulation, a fully structured mesh (see Figure 11) was implemented using growth factors from the surfaces to the simulation domain, thus allowing the refinement of grid elements close to the walls, as summarized in Table 6.

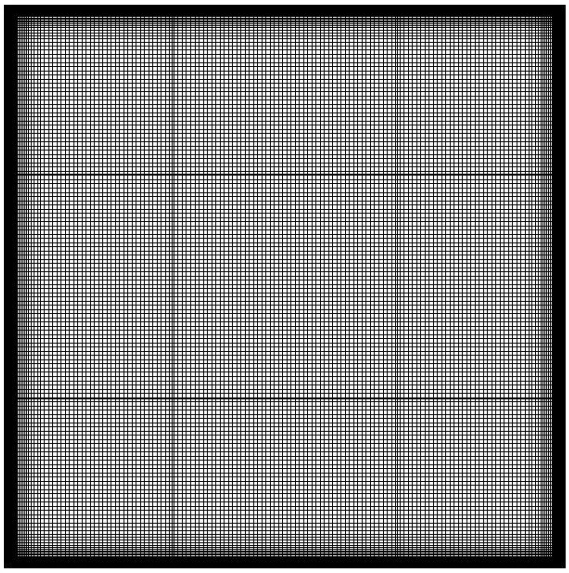

Figure 11: Visualization of the grid refinement close to the domain walls

Table 6: Main characteristics of the adopted grid spacing

Number of points on each wall [-]	750
Growth factor [-]	1.1
Maximum grid size [mm^2]	30

The very same circular flow pattern in the vertical middle plane, already determined using FDS, is visi-

ble in Figure 12. Again, velocity values in the central portion of the domain are negligible.

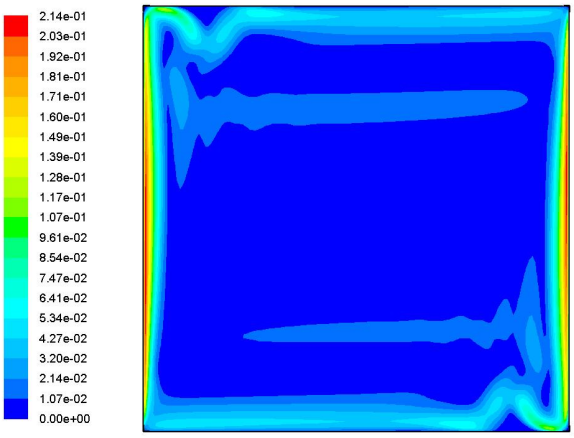

Figure 12: Example of flow pattern (scale of flow absolute velocity in m/s)

Figures from 13 to 16 show both the temperature and the vertical velocity profile at the middle line, as well as the specific convective heat transfer along both the hot and the cold walls respectively. A better approximation of the vertical velocity profile close to both hot and cold walls is clearly seen with respect to the simulation performed using FDS: this should be ascribed to a better near-wall grid resolution due to the adoption of the growth factors (and also to a more refined grid spacing, resulting from a 750x750 mesh). A marked improvement is also registered with respect to FDS as far as the prediction of the convective heat transfer is concerned.

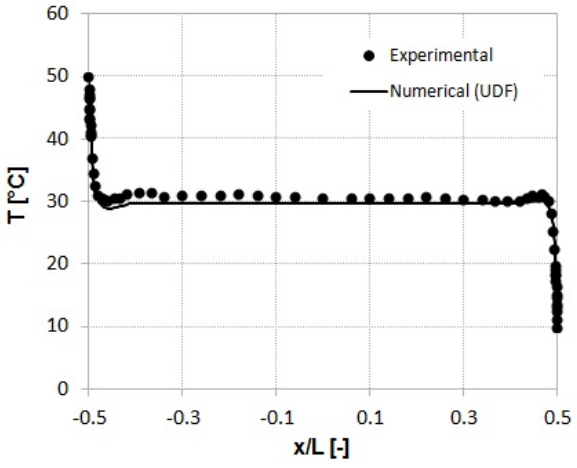

Figure 13: Temperature velocity profile at the middle line

The simulated peaks in the specific convective heat transfer along both the hot and the cold walls are

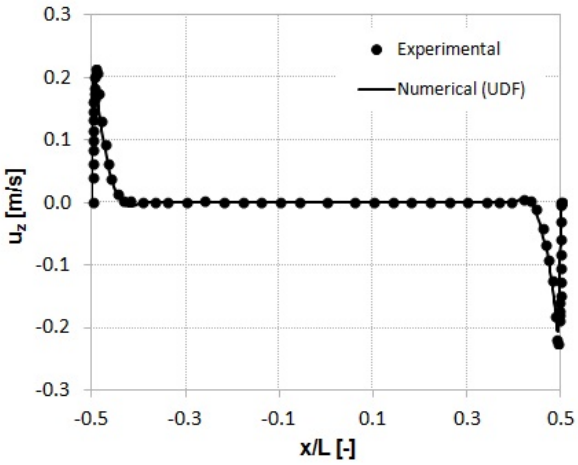

Figure 14: Vertical velocity profile at the middle line

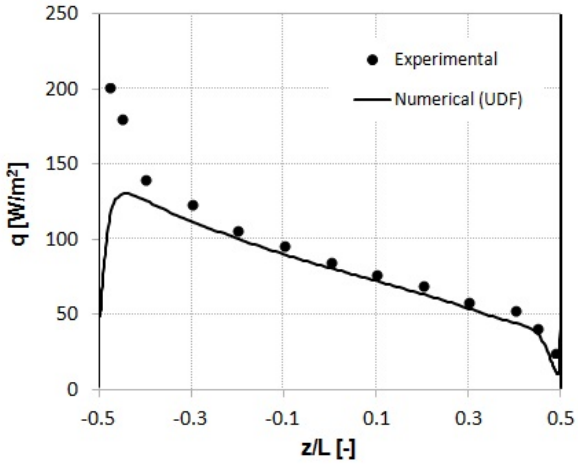

Figure 15: Specific convective heat transfer along the hot wall

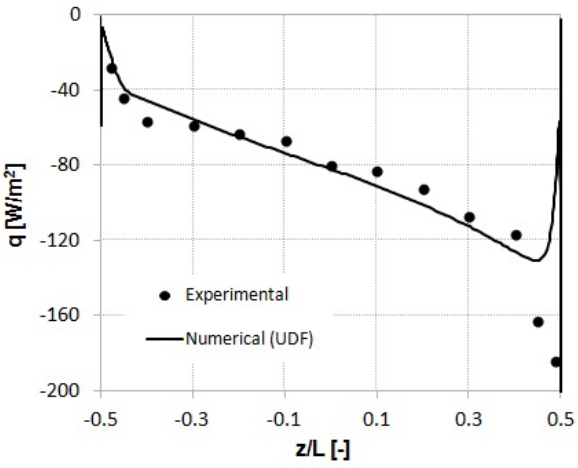

Figure 16: Specific convective heat transfer along the cold wall

to be ascribed to an incorrect temperature profiles imposed through the UDFs and deriving from temperature profiles stated in [8], which are probably not perfectly constant along the vertical walls.

7 Conclusions

It is well known that the LES approach proposed in FDS is quite convenient to reduce the calculation effort required for a CFD analysis. However, this approach implies significant approximations and the resulting code is optimized for a specific range of applications, that is fire scenarios in large enclosures.

However, even if the adoption of a widely accepted commercial code (Ansys Fluent) is still the best option for the simulation of buoyancy driven flows such as those occurring for natural convection in differentially heated square cavities filled by air, the FDS code can produce reliable results, provided that the correlations for the heat transfer on the walls are suitably modified. This conceptual result prompts for a future research aimed at defining the best wall correlation to be used in FDS, allowing to simulate natural and forced convection for different situations of common interest for designers.

References:

[1] S. Ostrach, Natural convection in enclosures, Journal of Heat Transfer, Vol. 110, Issue 4b (1988), pp. 1175-1190.

[2] J. Salat, S. Xin, P. Joubert, A. Sergent, F. Penot, P. Le Qur, Experimental and numerical investigation of turbulent natural convection in a large air-filled cavity, International journal of heat and fluid flow, Vol. 25, Issue 5 (2004), pp. 824-832.

[3] P. L. Betts, I. H. Bokhari, Experiments on turbulent natural convection in an enclosed tall cavity, International Journal of Heat and Fluid Flow, Vol. 21, Issue 6 (2000), pp. 675-683.

[4] Y. L., Chan, C. L. Tien, A numerical study of two-dimensional laminar natural convection in shallow open cavities, International Journal of Heat and Mass Transfer, Vol. 28, Issue 3 (1985), pp. 603-612.

[5] G. de Vahl Davis, Natural convection of air in a square cavity: a bench mark numerical solution, International Journal for Numerical Methods in Fluids, Vol. 3, Issue 3, (1983), pp. 249-264.

[6] T. Saitoh, K. Hirose, High-accuracy bench mark solutions to natural convection in a square cavity, Computational Mechanics, Vol. 4, Issue 6 (1989), pp. 417-427.

[7] P. Le Quere, Accurate solutions to the square thermally driven cavity at high Rayleigh number, Computers & Fluids, Vol. 20, Issue 1 (1991), pp. 29-41.

[8] F. Ampofo, T. G. Karayiannis, Experimental benchmark data for turbulent natural convection in an air filled square cavity, International Journal of Heat and Mass Transfer, 46 (2003), pp. 3551–3572.

[9] F. P. Incropera, D. P. De Witt, Fundamentals of Heat and Mass Transfer, John Wiley and Sons, New York, 4^{th} Edition, 1996.

[10] Y. Ji, M. J. Cook, V. Hanby, CFD modelling of natural displacement ventilation in an enclosure connected to an atrium, Building and Environment, Vol. 42, Issue 3 (2007), pp. 1158-1172.

[11] C. A. Rundlea, M. F. Lightstonea, P. Oosthuizenb, P. Karavac, E. Mourikid, Validation of computational fluid dynamics simulations for atria geometries, Building and Environment, Vol. 46, Issue 7 (2011), pp. 1343-1353.

[12] H. Manz, Numerical simulation of heat transfer by natural convection in cavities of facade elements, Energy and Buildings, Vol. 35, Issue 3 (2003), pp. 305-311.

[13] H. Yang, Z. Zhu, Numerical study of three-dimensional turbulent natural convection in a differentially heated air-filled tall cavity, International Communications in Heat and Mass Transfer, Vol. 35, Issue 5 (2008), pp 606-612.

[14] G. P. Mercier, Y. Jaluria, Fire-induced flow of smoke and hot gases in open vertical enclosures, Experimental thermal and fluid science, Vol. 19, Issue 2 (1999), pp 77-84.

[15] F. Penot, A. N'Dame, Successive bifurcations of natural convection in a vertical enclosure heated from the side, Third UK National Conference Incorporating First European Conference on Thermal Sciences, Birmingham (UK), Vol. 1 (1992), pp. 507513.

[16] Fire Dynamics Simulator Users Guide, NIST special publication 1019, 2014.

[17] J. Smagorinsky, General circulation experiments with the primitive equations: I. The basic experiment, Monthly Weather Review 91.3 (1963), pp. 99-164.

[18] S. B. Pope, Turbulent Flows, Cambridge University Press, 2000.

[19] H. Werner, H. Wengle, Large-eddy simulation of turbulent flow over and around a cube in a plate channel, 8^{th} Symposium on Turbulent Shear Flows (1991), Munich (Germany), pp. 155-168.

[20] J.P. Holman. Heat Transfer. McGraw-Hill, New York, 7^{th} Edition, 1990

[21] F. P. Incropera, D. P. De Witt, Fundamentals of Heat and Mass Transfer, John Wiley and Sons, New York, 4^{th} Edition, 1996.